

Fractional discrete vortex solitons

Cristian Mejía-Cortés¹ and Mario I. Molina²

¹*Programa de Física, Facultad de Ciencias Básicas,
Universidad del Atlántico, Puerto Colombia 081007, Colombia*

²*Departamento de Física, Facultad de Ciencias, Universidad de Chile, Casilla 653, Santiago, Chile*

(Dated: January 28, 2021)

We examine the existence and stability of nonlinear discrete vortex solitons in a square lattice when the standard discrete Laplacian is replaced by a fractional version. This creates a new, effective site-energy term, and a coupling among sites, whose range depends on the value of the fractional exponent α , becoming effectively long-range at small α values. At long-distance, it can be shown that this coupling decreases faster than exponential: $\sim \exp(-|\mathbf{n}|)/\sqrt{|\mathbf{n}|}$. In general, we observe that the stability domain of the discrete vortex solitons is extended to lower power levels, as the α coefficient diminishes, independently of their topological charge and/or pattern distribution.

Introduction. Vortices are objects characterized by a spatially-localized distribution of field intensities, together with a nontrivial phase distribution. This phase circulates around a singular point, or central core, changing by $2\pi S$ times in each closed loop around it (where S is an integer number). Integer S is known as the topological charge of the vortex. The sign of S determines the direction of power flow. In optics, this type of solution is also known as a vortex beam and has arisen considerable interest given their potential technological applications. Optical vortices have been envisioned as a mean to codify information using their topological charge value in classical [1] and quantum [2] regimes. Also, a stable vortex is capable of delivering its orbital angular momentum (OAM) to a nearby object, given way to one of its most remarkable applications: optical tweezers in biophotonics, where they are useful due to their ability to influence the motion of living cells, virus, and molecules [3–5]. Other applications can be found in optical systems communications [6] and spintronics [7].

A particular domain where discrete vortex solitons can be found, is in the discrete nonlinear Schrödinger (DNLS) equation [8–10], whose dimensionless form can be written as:

$$i \frac{dC_{\mathbf{n}}}{dt} + \sum_{\mathbf{m}} C_{\mathbf{m}} + \chi |C_{\mathbf{n}}|^2 C_{\mathbf{n}} = 0 \quad (1)$$

where $C_{\mathbf{n}}$ is, for instance, the amplitude of an optical or electronic field, χ is the nonlinear coefficient, and the sum is usually restricted to nearest-neighbor lattice sites. The DNLS equation has proven useful in describing a variety of phenomena in nonlinear physics, such as the transversal propagation of light in waveguide arrays [11–14], propagation of excitations in a deformable medium [15, 16], self-focusing and collapse of Langmuir waves in plasma physics [17, 18], dynamics of Bose-Einstein condensates inside coupled magneto-optical traps [19, 20], and description of rogue waves in the ocean [21], among others. Its main features include the existence of localized nonlinear solutions in 1D and 2D, usually referred to as discrete solitons, with families of stable and unstable states, the existence of a selftrapping transition [22, 23] of an initially localized excitation,

and a degree of excitation mobility in 1D [24]. For the DNLS equation, the existence and observation of discrete vortex solitons in Eq. (1) for several lattices have been reported in several works. For a square geometry and Kerr nonlinearity [Eq. (1)] it was found that the discrete vortex is stable when χ is larger than a critical value [25–27]. For saturable nonlinearity, discrete vortices have been experimentally observed in a square lattice [28]. They have also been studied in a nonlinear anisotropic Lieb lattice, which possesses a flat band [29]. For a hexagonal lattice in a self-focusing photorefractive crystal, vortices with $S = 1$ have been found but proven unstable, while for $S = 2$ a range of stability can be found [30–32]. Discrete vortices living at the boundary between a square and hexagonal lattice with photorefractive nonlinearity, have also been found [33].

Another field with substantial recent interest is that of fractional calculus. Its origin dates back to the firsts observations that the usual integer-order derivative could be extended to a fractional-order derivative, that is, $(d^n/dx^n) \rightarrow (d^\alpha/dx^\alpha)$, for real α , which is known as the fractional exponent. The field has a long history dating back to letters exchanged between L'Hopital and Leibnitz, followed by later contributions by Euler, Laplace, Riemann, Liouville, and Caputo, to name some. Several formalisms have been derived to treat these fractional derivatives, each one having its advantages and shortcomings. In the popular Riemann-Liouville formalism [34–37], the α -th derivative of a function $f(x)$ can be formally expressed as

$$\left(\frac{d^\alpha}{dx^\alpha}\right) f(x) = \frac{1}{\Gamma(1-\alpha)} \frac{d}{dx} \int_0^x \frac{f(x')}{(x-x')^\alpha} dx' \quad (2)$$

for $0 < \alpha < 1$. For the case of the laplacian operator $\Delta = \partial^2/\partial x^2 + \partial^2/\partial y^2$, its fractional form $(-\Delta)^\alpha$ in two dimensions can be expressed as [37]

$$(-\Delta)^\alpha f(\mathbf{x}) = L_{2,\alpha} \int \frac{f(\mathbf{x}) - f(\mathbf{y})}{|\mathbf{x} - \mathbf{y}|^{2+2\alpha}} \quad (3)$$

where,

$$L_{2,\alpha} = \frac{16 \Gamma(1+\alpha)}{\pi |\Gamma(-\alpha)|} \quad (4)$$

where $\Gamma(x)$ is the Gamma function and $0 < \alpha < 1$ is the fractional exponent.

The fractional Laplacian (3) has found many applications in fields as diverse as Levy processes in quantum mechanics [38], photonics [54], fractional kinetics and anomalous diffusion [39–41], strange kinetics [42], fluid mechanics [43, 44], fractional quantum mechanics [45, 46], plasmas [47], electrical propagation in cardiac tissue [48] and biological invasions [49].

In this work, we study the effect of replacing the usual two-dimensional discrete Laplacian by its fractional form [50, 51], on the creation and stability of discrete vortex solitons on a square lattice. As we will see, as the fractional exponent decreases, moving away from the usual non-fractional value, there is a stabilizing effect on those vortices with a topological charge equal to 2.

The model. Let us consider a square lattice, where the kinetic energy term in Eq.(1), $\sum_{\mathbf{m}} C_{\mathbf{m}}$, can be written as $4C_{\mathbf{n}} + \Delta_n C_{\mathbf{n}}$, where Δ_n corresponds a the well-known

expression for the discretized Laplacian

$$\Delta_n C_{\mathbf{n}} = C_{p+1,q} + C_{p-1,q} - 4 C_{p,q} + C_{p,q+1} + C_{p,q-1}, \quad (5)$$

where $\mathbf{n} = (p, q)$. Equation (1) can then rewritten as

$$i \frac{dC_{\mathbf{n}}}{dt} + 4C_{\mathbf{n}} + \Delta_n C_{\mathbf{n}} + \chi |C_{\mathbf{n}}|^2 C_{\mathbf{n}} = 0. \quad (6)$$

Let us now replace the Laplacian Δ_n by its fractional form $(\Delta_n)^\alpha$, and given by [52, 53]

$$(\Delta_n)^\alpha C_{\mathbf{n}} = \sum_{\mathbf{m} \neq \mathbf{n}} (C_{\mathbf{m}} - C_{\mathbf{n}}) K^\alpha(\mathbf{n} - \mathbf{m}) \quad (7)$$

where,

$$K^\alpha(\mathbf{m}) = \frac{1}{|\Gamma(-\alpha)|} \int_0^\infty e^{-4t} I_{m_1}(2t) I_{m_2}(2t) t^{-1-\alpha} dt \quad (8)$$

with $\mathbf{m} = (m_1, m_2)$ and $I_m(x)$ is the modified special Bessel function. An equivalent expression for $(\Delta_n)^\alpha$ is

$$(\Delta_n)^\alpha C_{\mathbf{j}} = L_{2,\alpha} \sum_{\mathbf{m} \neq \mathbf{j}} (C_{\mathbf{m}} - C_{\mathbf{j}}) G_{3,3}^{2,2} \left(\begin{matrix} 1/2, -(j_2-m_2+1+\alpha, j_2-m_2+1+\alpha) \\ 1/2+\alpha, j_1-m_1, -(j_1-m_1) \end{matrix} \middle| 1 \right) \quad (9)$$

where $\mathbf{j} = (j_1, j_2)$ and $\mathbf{m} = (m_1, m_2)$, and $G(\dots)$ is the Meijer G-function. As we can see, the symmetric kernel $K^\alpha(\mathbf{m}) = K^\alpha(-\mathbf{m})$ plays the role of a long-ranged coupling. Near $\alpha = 1$, $K(\mathbf{m}) \rightarrow \delta_{\mathbf{m},\mathbf{u}}$ where $\mathbf{u} = (1, 0)$ or $\mathbf{u} = (0, 1)$, i.e., coupling to nearest neighbors only. Equation (6) can now be written as

$$i \frac{dC_{\mathbf{n}}}{dt} + 4C_{\mathbf{n}} + \sum_{\mathbf{m} \neq \mathbf{n}} (C_{\mathbf{m}} - C_{\mathbf{n}}) K^\alpha(\mathbf{m} - \mathbf{n}) + \chi |C_{\mathbf{n}}|^2 C_{\mathbf{n}} = 0, \quad (10)$$

With a bit of algebraic manipulations, it is possible to prove that Eq.(10) has two conserved quantities namely, the power

$$P = \sum_{\mathbf{n}} |C_{\mathbf{n}}(t)|^2 \quad (11)$$

and the Hamiltonian,

$$H = \sum_{\mathbf{n}} (4 - \sum_{\mathbf{m} \neq \mathbf{n}} K^\alpha(\mathbf{n} - \mathbf{m})) |C_{\mathbf{n}}|^2 + \sum_{\mathbf{n}} \sum_{\mathbf{m} \neq \mathbf{n}} K^\alpha(\mathbf{n} - \mathbf{m}) C_{\mathbf{n}}^* C_{\mathbf{m}} + (\chi/2) \sum_{\mathbf{n}} |C_{\mathbf{n}}|^4. \quad (12)$$

These relations prove useful when monitoring the accuracy of numerical computations.

Now let us consider stationary modes defined by $C_{\mathbf{n}}(t) = e^{i\lambda t} \phi_{\mathbf{n}}$, which obey

$$(-\lambda + 4) \phi_{\mathbf{n}} + \sum_{\mathbf{m} \neq \mathbf{n}} (\phi_{\mathbf{m}} - \phi_{\mathbf{n}}) K^\alpha(\mathbf{m} - \mathbf{n}) + \chi |\phi_{\mathbf{n}}|^2 \phi_{\mathbf{n}} = 0, \quad (14)$$

where $\phi_{\mathbf{n}}$ is the field amplitude that defines a complex spatial profile of the solution, and λ is the propagation constant.

It should be mentioned that, when dealing with a finite square lattice, in expressions (6) and (14) the term 4 is to be replaced by 3 (2) when \mathbf{n} falls at the edge (corner). Figure 1 shows the effective site energy $\epsilon(\mathbf{n}) = 4 - \sum_{\mathbf{m} \neq \mathbf{n}} K^\alpha(\mathbf{m} - \mathbf{n})$ and effective coupling $K^\alpha(\mathbf{m} - \mathbf{n})$. We can see that, as α decreases, the range of the coupling between two distant sites increases. In particular, for $\mathbf{n} = 0$ and along the main diagonal $\mathbf{m} = (m, m)$, its value can be shown to approach

$$K^\alpha(m) \sim \frac{1}{|\Gamma(-\alpha)|} \frac{2^{-2m}}{\sqrt{m}} \quad (n \rightarrow \infty), \quad (15)$$

i.e., faster than exponential.

Discrete vortex solitons. Let us examine the non-linear stationary modes given as complex solutions of Eq.(14) and characterized by a nontrivial distribution of the phases. They form a set of $N \times N$ nonlinear algebraic equations for the amplitudes $\{C_{\mathbf{n}}\}$. The form of the nonlinear term chosen here is of the Kerr type (cubic), although other forms can be used, such as the saturable nonlinearity[29]. Numerical solutions are obtained by the use of a multidimensional Newton-Raphson scheme, using as a seed a solution in the form $C_{\mathbf{n}} = A_{\mathbf{n}} \exp(iS\theta_{\mathbf{n}})$, where S is the topological charge and θ is the azimuthal angle of the n th site, with a highly localized distribu-

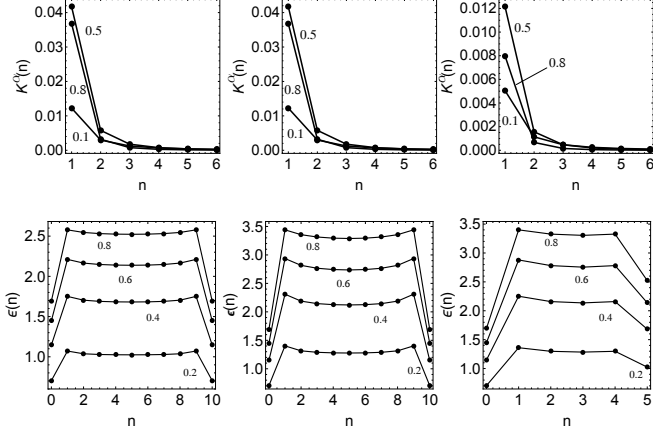


Figure 1. First row: Effective coupling $K^\alpha(\mathbf{n} - \mathbf{m})$ between $\mathbf{m} = (0, 0)$ and sites $\mathbf{n} = (n, 0)$ (left column), $\mathbf{n} = (n, n)$ (middle column), and $\mathbf{n} = (n, 2n)$ (right column). Second row: Effective site energy $\epsilon(\mathbf{n})$ for several fractional exponents α and $\mathbf{n} = (n, 0)$ (left column), $\mathbf{n} = (n, n)$ (middle column), and $\mathbf{n} = (n, 2n)$ (right column). Number of sites = 10×10 . The numbers on each curve denote the value of the fractional exponent.

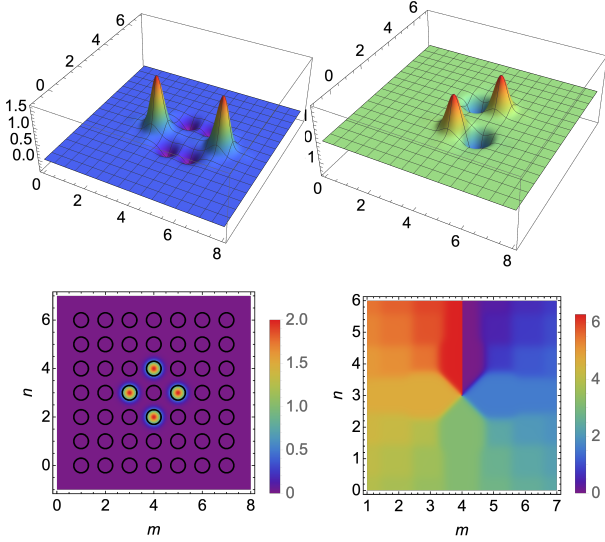


Figure 2. 4-sites discrete vortex with $S = 1$ and exponent $\alpha = 0.2$. (a) Real part (b) Imaginary part (c) Amplitude profile (d) Phase profile. ($\lambda = 6$)

tion for A_n . This ansatz is obtained from the decoupled limit, also known as the anticontinuous limit, where each site becomes decoupled from each other. We use a finite $N \times N$ lattice with open boundary conditions. Figures 2 and 3 show examples of two different discrete vortex solitons with fractional exponent $\alpha = 0.2$, and two val-

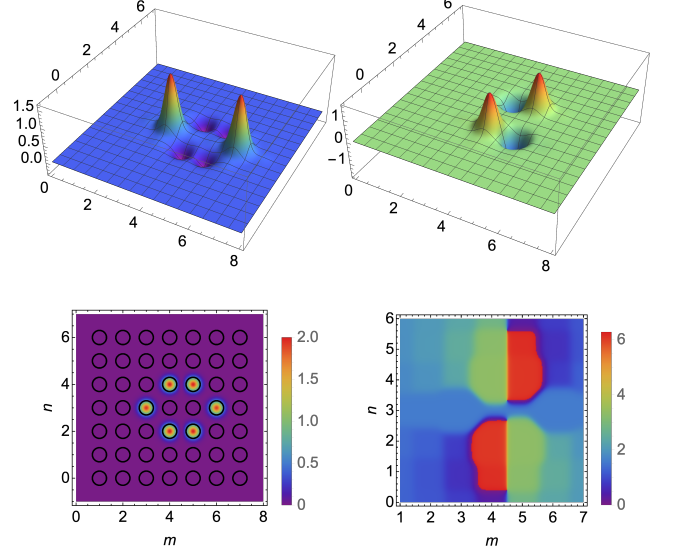


Figure 3. 6-sites discrete vortex with $S = 2$ and exponent $\alpha = 0.2$. (a) Real part (b) Imaginary part (c) Amplitude profile (d) Phase profile. ($\lambda = 6$)

ues of the topological charge, $S = 1$ and $S = 2$. As we will show, the main effect of small α values of fractionality is to stabilize the modes with $S = 2$ with 4 and 6 sites, while inhibiting the existence of modes with $S = 1$ modes for the 6-sites mode. At α values in the range $0.5 < \alpha < 1$, fractionality does not seem to affect the stability of the $S = 1$ mode. For the modes with $S = 1$ and 4 sites, stability is not affected by fractionality.

The stability of the computed vortex solitons is carried out by a simple linear stability analysis, which we describe briefly here for completeness. We start by perturbing the vortex solution $C_n = (\phi_n + \delta_n) \exp(i\lambda t)$, where ϕ_n is the solution of Eq.(14) and $|\delta_n(t)| \ll |\phi_n|$. We replace this in the evolution equation (6) [with Δ_n replaced by its fractional form $(\Delta_n)^\alpha$]. After a linearization procedure, where we neglect any powers of $\delta_n(t)$ beyond the linear one, we obtain a set of linear evolution equations for $\delta_n(t)$. Next, we decompose $\delta_n(t)$ into its real and imaginary parts: $\delta_n(t) = x_n(t) + i y_n(t)$. To simplify the notation we map the sites of the two-dimensional square lattice into those of an open one-dimensional chain: $(n_1, n_2) \rightarrow n \equiv n_1 + (n_2 - 1)N$, with $1 \leq n_1, n_2 \leq N$. Then, the equations for $x_n(t)$ and $y_n(t)$ can be written in the form:

$$\frac{d^2}{dt^2} \vec{x} - \mathbf{A} \mathbf{B} \vec{x} = 0, \quad \frac{d^2}{dt^2} \vec{y} - \mathbf{B} \mathbf{A} \vec{y} = 0, \quad (16)$$

where $\vec{x} = (x_1, x_2, \dots, x_{N \times N})$ and $\vec{y} = (y_1, y_2, \dots, y_{N \times N})$. Matrices \mathbf{A} and \mathbf{B} are given by

$$\mathbf{A}_{nm} = [-\lambda - K^\alpha(0) + \epsilon_n + \chi(2|\phi_n|^2 - \phi_n^2)] \delta_{nm} + K^\alpha(n-m) \quad (17)$$

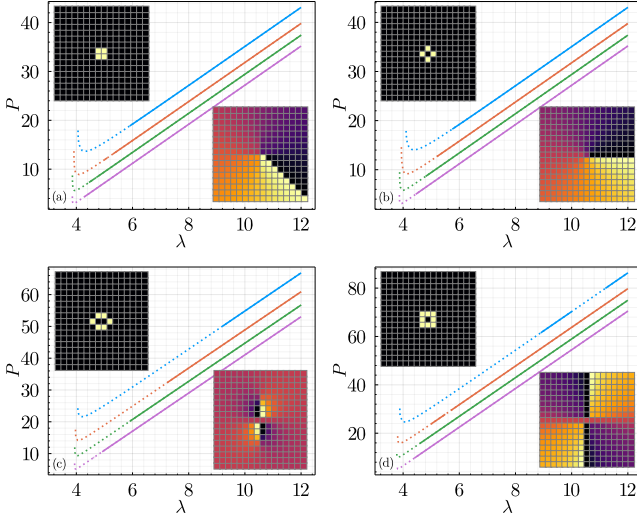


Figure 4. Power content versus eigenvalue of some vortex solitons, for several fractional exponents and topological charges $S = 1$ (upper row) and $S = 2$ (lower row). Solid (dashed) lines represent stable (unstable) solutions. Blue, orange, green and violet lines correspond to $\alpha = 0.8, 0.6, 0.4$ and 0.2 , respectively. Amplitude (top left) and phase profile (bottom right) at inset of each diagram corresponds to solutions for $\lambda = 12$.

$$\mathbf{B}_{nm} = [\lambda + K^\alpha(0) - \epsilon_n - \chi(2|\phi_n|^2 + \phi_n^2)] \delta_{nm} - K^\alpha(n-m) \quad (18)$$

where $\epsilon_n = \beta - \sum_j K^\alpha(n-j)$, with $\beta = 2$ for a corner site, $\beta = 3$ for an edge site, and $\beta = 4$ for a bulk site (in solid state physics, β is known as the coordination number). Linear stability is determined from the eigenvalue spectra of the matrices \mathbf{AB} (or \mathbf{BA}). When all eigenvalues are real and negative (positive), the system is stable (unstable). In the more general case that also considers possible complex eigenvalues, one defines the instability gain G as:

$$G = \text{Max of} \left\{ \frac{1}{2} \left(\text{Re}(g) + \sqrt{\text{Re}(g)^2 + \text{Im}(g)^2} \right) \right\}^{1/2} \quad (19)$$

for all g , where g is an eigenvalue of \mathbf{AB} (\mathbf{BA}). Thus, when $G = 0$, the mode under inspection is stable; otherwise it is unstable.

Results from the above procedure are displayed in Fig. 4. They are summarized by mean of P vs λ diagrams, for several values of the fractional exponent α . Amplitude (top left) and phase (bottom right) profiles for these kinds of stationary vortex solutions are displayed at the inset of each diagram. We see that vortex beams with $S = 1$ and four main peaks, the off-site square (a) and diamond shape (b), increase their stability domain as the α coefficient diminish. Similar behavior can be observed for those stationary modes endowed with $S = 2$ and displaying six main peaks and hexagonal shape (c). However, for modes with eight peaks and on-site square

shape (d), the stability domain displays a piecewise domain for high values of α . Here, we have employed a $N \times N$ square lattice with $N = 17$. As normally happens in the non-fractional case, families of modes, indistinct of α coefficient, exhibit a saddle-node bifurcation near to the linear band border. Here we only calculate solutions belonging to the lower branch of the bifurcation point. Discrete solitons display here highly localized patterns, as expected for a cubic nonlinearity. We can observe a smooth spiral phase for any loop enclosing the singularity, in those solutions with symmetric amplitude profiles matching their nominal topological charge. On the contrary, for the hexagonal asymmetric pattern, the topological charge only can be observable in the region where the field amplitude is significant.

In all cases, without exception, the power curves shift down as α is decreased. Another observation concerns the limit $s \rightarrow 0$. In that limit, the range of the coupling diverges and, as a result, all sites are coupled with each other. Assuming that the amplitude at each site is nearly identical, the stationary equations (14) reduce to $(-\lambda + 4)\phi + \chi\phi^3 \approx 0$. For $\phi \neq 0$ we have $(4 - \lambda) + \chi\phi^2 \approx 0$. Using $P \sim Z\phi^2$ where Z is the number of sites initially excited, we have $P \approx (Z/\chi)(\lambda - 4)$. For $\lambda < 4$, we must take $\phi = 0$, which implies $P = 0$. This linear dependence can be clearly seen in all plots of Fig.4 at small α values.

Conclusions. In this work we considered the existence and stability of discrete vortex solitons of the discrete nonlinear Schrödinger (DNLS) equation, when the usual Laplacian $\Delta_{\mathbf{n}}$ is replaced by a fractional version $(\Delta_{\mathbf{n}})^\alpha$ with $0 < \alpha < 1$. We employed a square lattice and a Kerr nonlinearity and computed discrete vortex modes and their stability for different values of the fractional exponent α . Discrete vortex solitons reported here, namely, the diamond, off and on-site square and hexagonal shape, exist for any value of fractional exponent and $S = 1$ and $S = 2$ topological charges. However, those with diamond and off-site square shape, are only stable for $S = 1$. On the contrary, the on-site square and hexagonal shape cases are stable for $S = 2$. The existence and stability of these modes are strongly related to their spatial distribution, as well as to the lattice geometry. In all cases examined, a decrease of the fractional exponent α causes the power stability curves to shift to lower values.

In general, the basic properties of discrete vortices observed before for the standard Laplacian exponent ($\alpha = 2$) are more or less maintained in the case a fractional Laplacian. This is in itself interesting, since it suggests that the discrete vortex soliton properties are robust against mathematical “perturbations”.

ACKNOWLEDGMENTS

This work was supported by Fondecyt Grant 1200120.

-
- [1] G. Molina-Terriza, J. P. Torres, and L. Torner, Management of the angular momentum of light: Preparation of photons in multidimensional vector states of angular momentum, *Phys. Rev. Lett.* 88, 013601 (2001).
 - [2] A. Mair, A. Vaziri, G. Weihs, and A. Zeilinger, Entanglement of the orbital angular momentum states of photons, *Nature*. 412, 313-316 (2001)
 - [3] Andy Chong, Chenhao Wan, Jian Chen, Qiwen Zhan, Generation of spatiotemporal optical vortices with controllable transverse orbital angular momentum, *Nature Photonics*. 14, 350-354 (2020)
 - [4] X. Zhuang, Unraveling dna condensation with optical tweezers, *Science*. 305, 188-190 (2004).
 - [5] I. A. Favre-Bulle, A. B. Stilgoe, E. K. Scott, and H. Rubinsztein-Dunlop, Optical trapping in vivo: theory, practice, and applications, *Nanophotonics*. 8, 1023-1040 (2019).
 - [6] J. T. Barreiro, T.-C. Wei, and P. G. Kwiat, Beating the channel capacity limit for linear photonic superdense coding, *Nat. Phys.* 4, 282-286 (2008).
 - [7] S. D. Ganichev, E. L. Ivchenko, S. N. Danilov, J. Eroms, W. Wegscheider, D. Weiss, and W. Prettl, Conversion of spin into directed electric current in quantum wells, *Phys. Rev. Lett.* 86, 4358-4361 (2001).
 - [8] P. G. Kevrekidis, *The Discrete Nonlinear Schrödinger Equation* (Springer, Berlin Heidelberg 2009).
 - [9] J. C. Eilbeck, P. S. Lomdahl, and A. C. Scott. The discrete selftrapping equation, *Physica D* 16 (1985) 318-338.
 - [10] J. C. Eilbeck, M. Johansson, The discrete nonlinear Schrödinger equation-20 years on, *Proceedings of the Conference on Localization and Energy Transfer in Nonlinear Systems*, Madrid, Spain (2002). (World Scientific, 2003).
 - [11] D. N. Christodoulides, R. I. Joseph, Discrete self-focusing in nonlinear arrays of coupled waveguides, *Optics letters* 13 (1988) 794-796.
 - [12] F. Lederer, G. I. Stegeman, D. N. Christodoulides, G. Assanto, M. Segev, Y. Silberberg, Discrete solitons in optics, *Physics Reports* 463 (2008) 1-126.
 - [13] Rodrigo A. Vicencio, Mario I. Molina, and Yuri S. Kivshar, *Phys. Rev. E* 70 (2004) 026602.
 - [14] J. W. Fleischer, M. Segev, N.K. Efremidis, D.N. Christodoulides, Observation of two-dimensional discrete solitons in optically induced nonlinear photonic lattices, *Nature* 422 (2003) 147-150.
 - [15] A. S. Davydov, Solitons and energy transfer along protein molecules, *J. Theor. Biology* 66 (1977) 379-387.
 - [16] P. L. Christiansen and A. C. Scott (Eds). *Davydov's Soliton Revisited: Self-trapping of Vibrational Energy in Protein* (Plenum Press, New York, 1990).
 - [17] V.E. Zakharov, Collapse and self-focusing of Langmuir waves, in: *Handbook of Plasma Physics*, Vol. 2, Basic Plasma Physics, eds. A.A. Galeev, R.N. Sudan, (Elsevier North-Holland 1984), pp. 81-121.
 - [18] V. E. Zakharov, Collapse of Langmuir Waves, *Sov. Phys. JETP* 35 (1972) 908-914.
 - [19] O. Morsh, M. Oberthaler, Dynamics of Bose-Einstein condensates in optical lattices, *Rev. Mod. Phys.* 78 (2006) 179-215.
 - [20] V. A. Brazhnyi, V. V. Konotop, Theory of nonlinear matter waves in optical lattices, *Mod. Phys. Lett. B* 18 (2004) 627-651.
 - [21] M. Onorato, A. R. Osborne, M. Serio, S. Bertone, Freak Waves in Random Oceanic Sea States, *Phys. Rev. Lett.* 86 (2001) 5831.
 - [22] M. I. Molina, G. P. Tsironis, Dynamics of self-trapping in the discrete nonlinear Schrödinger equation, *Physica D* 65 (1993) 267-273.
 - [23] G. P. Tsironis, W. D. Deering, M. I. Molina, Applications of self-trapping in optically coupled devices, *Physica D* 68 (1993) 135-137.
 - [24] Rodrigo A. Vicencio, Mario I. Molina, and Yuri S. Kivshar, Switching of discrete optical solitons in engineered waveguide arrays, *Phys. Rev. E* 70 (2004) 026602.
 - [25] B. A. Malomed and P. G. Kevrekidis, Discrete vortex solitons, *Phys. Rev. E* 64, 026601 (2001).
 - [26] D. N. Neshev, T. J. Alexander, E. A. Ostrovskaya, Y. S. Kivshar, H. Martin, I. Makasyuk, and Z. Chen, Observation of Discrete Vortex Solitons in Optically Induced Photonic Lattices, *Phys. Rev. Lett.* 92, 123903 (2004).
 - [27] E. Arevalo, Soliton Theory of Two-Dimensional Lattices: The Discrete Nonlinear Schrödinger Equation, *Phys. Rev. Lett.* 102, 224102 (2009).
 - [28] J.W. Fleischer, G. Bartal, O. Cohen, Observation of vortex-ring discrete solitons in 2D photonic lattices, *Phys. Rev. Lett.* 92 (2004) 123904.
 - [29] Cristian Mejía-Cortés, Jorge Castillo-Barake and Mario I. Molina, "Discrete vortex solitons in the anisotropic Lieb lattice", *Opt. Lett.* 45, 3569 (2020).
 - [30] L.J.H. Law, P.G. Kevrekidis, T.J. Alexander, W. Krolikowski, Y.S. Kivshar, Stable higher-charge discrete vortices in hexagonal optical lattices, *Phys. Rev. A* 79 (2009) 025801.
 - [31] H. Leblond, B.A. Malomed, D. Mihalache, Spatiotemporal vortex solitons in hexagonal arrays of waveguides, *Phys. Rev. A* 83 (2011) 063825.
 - [32] B. Terhalle, T. Richter, K.J.H. Law, D. Göries, P. Rose, T.J. Alexander, P.G. Kevrekidis, A.S. Desyatnikov, W. Krolikowski, F. Kaiser, C. Denz, Y.S. Kivshar, Observation of double-charge discrete vortex solitons in hexagonal photonic lattices, *Phys. Rev. A* 79 (2009) 043821.
 - [33] D.J. Savic, A. Piper, R. Zikic, D. imotijevic, Vortex solitons at the interface separating square and hexagonal lattices, *Phys. Lett. A* 379 (2015) 1110?1113
 - [34] R. Herrmann, *Fractional Calculus - An Introduction for Physicists* (World Scientific Singapore 2014).
 - [35] Bruce West, Mauro Bologna, Paolo Grigolini, *Physics of Fractal Operators*, (Springer 2003).
 - [36] *An Introduction to the Fractional Calculus and Fractional Differential Equations*, por Kenneth S. Miller, Bertram Ross (Ed.) (John Wiley & Sons 1993).
 - [37] N.S. Landkof, *Foundations of Modern Potential Theory* (Translated from the Russian by A.P. Doohovskoy), *Die Grundlehren der mathematischen Wissenschaften*, vol. 180, (Springer-Verlag New York 1972).
 - [38] N. C. Petroni and M. Pusterla, Levy processes and Schrodinger equation, *Physica A* 388, 824 (2009).
 - [39] R. Metzler, J. Klafter, The random walk's guide to anomalous diffusion: a fractional dynamics approach, *Phys. Rep.* 339 (2000) 1-77.
 - [40] I. M. Sokolov, J. Klafter and A. Blumen, Fractional kinetics, *Physics Today* 55, 44-58 (2002).

- [41] G. M. Zaslavsky, Chaos, fractional kinetics, and anomalous transport, *Phys. Rep.* **371** (2002), 461-580.
- [42] M. F. Shlesinger, G. M. Zaslavsky and J. Klafter, Strange kinetics, *Nature* **363** (1993), 31-37.
- [43] L. A. Caffarelli, A. Vasseur, Drift diffusion equations with fractional diffusion and the quasi-geostrophic equation, *Ann. of Math.* **171** (2010) 1903-1930.
- [44] P. Constantin and M. Ignatova, Critical SQG in bounded domains, *Ann. PDE* **2** (2016) 1-42.
- [45] N. Laskin, Fractional quantum mechanics, *Phys. Rev. E* **62** (2000) 3135. (2000).
- [46] N. Laskin, Fractional Schrodinger equation, *Phys. Rev. E* **66**, 056108 (2002).
- [47] M. Allen, A fractional free boundary problem related to a plasma problem, *Comm. Anal. Geom.* **27**, 1665 (2019).
- [48] A. Bueno-Orovio, D. Kay, V. Grau, B. Rodriguez and K. Burrage, Fractional diffusion models of cardiac electrical propagation: role of structural heterogeneity in dispersion of repolarization, *Journal of The Royal Society Interface* **11(97)**, 20140352 (2014).
- [49] H. Berestycki, J.-M. Roquejoffre and L. Rossi, The influence of a line with fast diffusion on Fisher-KPP propagation, *J. Math. Biol.* **66** (2013) 743.
- [50] M. I. Molina, The Fractional Discrete Nonlinear Schrödinger Equation, M. I. Molina, *Phys. Lett. A* **384**, 126180 (2020).
- [51] M. I. Molina, The Two-Dimensional Fractional Discrete Nonlinear Schroedinger Equation, *Phys. Lett. A* **384**, 126835 (2020).
- [52] Oscar Ciaurri, Luz Roncal, Pablo Raul Stinga, Jose L. Torrea, Juan Luis Varona, Nonlocal discrete diffusion equations and the fractional discrete Laplacian, regularity and applications, *Advances in Mathematics* **330** (2018) 688.
- [53] Luz Roncal, private communication.
- [54] Xiankun Yao, Xueming Liu, Off-site and on-site vortex solitons in space-fractional photonic lattices, *Opt. Lett.* **43**, 5749-5752 (2018)